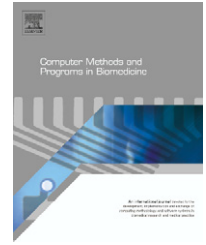




ELSEVIER

journal homepage: www.intl.elsevierhealth.com/journals/cmpb

Sensitivity study of human crystalline lens accommodation

A. Abolmaali^a, R.A. Schachar^{b,*}, T. Le^a

^a Department of Civil and Environmental Engineering, University of Texas at Arlington, TX 76019, USA

^b Physics Department, University of Texas at Arlington, PO Box 601149, Dallas, TX 75360, USA

ARTICLE INFO

Article history:

Received 9 June 2006

Received in revised form

22 August 2006

Accepted 24 August 2006

Keywords:

Quadrilateral elements

Human crystalline lens

accommodation

Nonlinear finite element analysis

Sensitivity study

Mixed formulation finite element modeling

ABSTRACT

A nonlinear axisymmetric finite element method (FEM) analysis was employed to determine the critical geometric and material properties that affect human accommodation. In this model, commencing at zero, zonular traction on all lens profiles resulted in central lenticular surface steepening and peripheral surface flattening, with a simultaneous increase in central lens thickness and central optical power. An age-related decline in maximum zonular tension appears to be the most likely etiology for the decrease in accommodative amplitude with age.

© 2006 Elsevier Ireland Ltd. All rights reserved.

1. Introduction

The young human eye can rapidly change optical power by altering the shape of its crystalline lens. The induced change in focal length is called accommodation and is measured in diopters; i.e., the inverse of the focal length in meters.

The crystalline lens is axisymmetric with a mid-sagittal profile similar to an ellipse with minor (central thickness) and major diameters (equatorial diameter) of approximately 4 and 9 mm, respectively. The lens consists of 35% protein and 65% water. It is totally transparent and enclosed in a thin membrane capsule. The lens is located behind the iris approximately 3 mm from the apex of the cornea with its axis of symmetry approximately coincident with the optical axis of the eye. It is suspended in the eye between the aqueous humor and the vitreous body by zonular fibers that are inserted into the equatorial region of the lens capsule. The zonular fibers originate in the ciliary body and transduce the force of con-

traction of the ciliary muscle to the lens capsule. Contraction of the ciliary muscle induces lenticular accommodation.

The mechanisms of lenticular accommodation and its age-related loss continue to be of great interest [1]. The amplitude of human accommodation declines at the approximate rate of 0.25 diopters/year. By the mid-forties, the near point of vision is more distant than that required for reading. When this occurs, the patient has demonstrated presbyopia [2,3]. By the age of 50, little residual ability to change focus remains.

Unfortunately, direct, *in vivo*, measurement of most of the geometric and material properties of the whole human lens is not possible. Alternative approaches are, therefore, needed to characterize and understand the mechanism of lenticular accommodation and its change with aging.

The finite element method (FEM) coupled with a sensitivity study is a reliable method for determining the critical physiological factors that affect biological tissues [4–6]. In a sensitivity study, the geometric and material properties are varied

* Corresponding author. Tel.: +1 214 695 0080; fax: +1 214 368 5970.

E-mail address: ron@2ras.com (R.A. Schachar).

0169-2607/\$ – see front matter © 2006 Elsevier Ireland Ltd. All rights reserved.

doi:10.1016/j.cmpb.2006.08.005

to determine the physiological limits of each variable within the constraints of the system [7–10]. The present study uses a sensitivity study to establish the physiologic range for the geometric and material properties of the lens and their effect on the mechanism of accommodation and its age-related decline.

Several analyses of human lenticular accommodation have been published using nonlinear FEM [11–15]. However, the present FEM analysis differs markedly from these prior studies in several important ways. This analysis is a sensitivity study, using quadrilateral elements to represent the capsule, surface-to-surface contact elements between the capsule and cortex, and satisfying all of the constraints on the force, topography and anatomy of human lenticular accommodation.

2. FEM model

2.1. Baseline geometric properties

It has not yet been possible to determine, *in vivo*, the human lens shape at high resolution. The available magnetic resonance images (MRI) of *in vivo* entire human lens profiles have resolutions that are less than 150 μm . This limitation in resolution makes current MRI images insufficient to delineate the exact radius of curvature of the lens surfaces.

In order to address this limitation, our model employs a function for the anterior and posterior surface of the baseline lens that best fits the available MRI profile of the whole lens. This function is continuous and has the following essential requirements:

1. The radii of curvatures at any point on the lens surface are smoothly varied.
2. The radii do not change abruptly near the optical axis.
3. The radii are identical at the equator where the anterior and posterior surfaces meet.

4. The functions have a positive Gaussian curvature everywhere on the surface.

This function is [16]:

$$y(x) = \left[b + c \left(\sin^{-1} \left(\frac{x}{a} \right) \right)^2 + d \left(\sin^{-1} \left(\frac{x}{a} \right) \right)^4 \right] \times \cos \left(\sin^{-1} \left(\frac{x}{a} \right) \right) \quad (2.1)$$

The lens profiles, profiles I and II [17]; profile III [18] and profiles IV and V [19] were obtained from published MRI images. The coefficients employed in Eq. (2.1) for each lens profile are given in Table 1. The capsular thickness variation was incorporated in all profiles using the functions given by Chien et al. [16]. The thickness of the center of the anterior and posterior capsules, at baseline, was 24 and 5 μm , respectively [20,21]. The thickness of the nucleus of the lens model was calculated as a percentage of its central lens thickness (CLT), based on *in vivo* Scheimpflug measurements [22] (Fig. 1a, Table 1).

2.2. Baseline material properties

2.2.1. Lens stroma (cortex and nucleus)

The bulk modulus, K , of the human lens cortex and nucleus is 2.8 and 3.7 GPa, respectively [23], as measured by non-invasive Brillouin light scattering. These bulk moduli determined *in vitro*, are consistent with those calculated *in vivo*, using the speed of ultrasound in young human lenses [24], and the density of the lens [25].

Pieces of young adult human lenses (14–25 years of age), stored in liquid nitrogen, were used to determine the mean shear modulus, $G=50\text{ Pa}$ [26]. The Poisson's ratio, ν , and the elastic modulus are related to K and G by the following

Table 1 – Geometrical properties of the lenses

	Profile I	Profile II	Profile III	Profile IV	Profile V	Idealized
Coefficients for anterior profile Eq. (1) (mm)						
a	4.485	4.2815	4.5	4.5	4.3	4.3
b	1.2089032	1.463629	1.55467	1.439666869	1.75102	1.9
c	-0.266892	-0.166822	-0.329	-0.0962011	-0.130361	0.1795833
d	0.1166546	-0.021135	0.08141	0.11257732	0.117481	-0.3848683
Coefficients for posterior profile Eq. (1) (mm)						
a	4.485	4.2815	4.5	4.5	4.3	4.3
b	2.1669011	2.260218	2.27038	2.377780173	2.628273	2.00
c	-0.368996	-0.259828	-0.6326	-0.58929807	-0.964052	-0.192903226
d	0.0006791	-0.114285	0.0869	0.158321934	0.311269	-0.25033071
Dimensions for the lens outline (see Fig. 1b) (mm)						
a	4.485	4.2815	4.5	4.5	4.3	4.3
e	0.3570	0.3938	0.4045	0.4037	0.4631	0.4045
f	2.5565	2.4405	2.3850	2.7900	2.6660	2.8504
g	0.8768	1.0232	1.1352	0.9508	1.1285	0.9714
h	1.9242	2.1226	2.0273	2.3668	2.7152	2.4180
i	1.2089	1.4636	1.5547	1.4397	1.7510	1.900
j	2.1669	2.2602	2.2704	2.3778	2.6283	2.000
t	3.3758	3.7238	3.8250	3.8174	4.3793	3.900

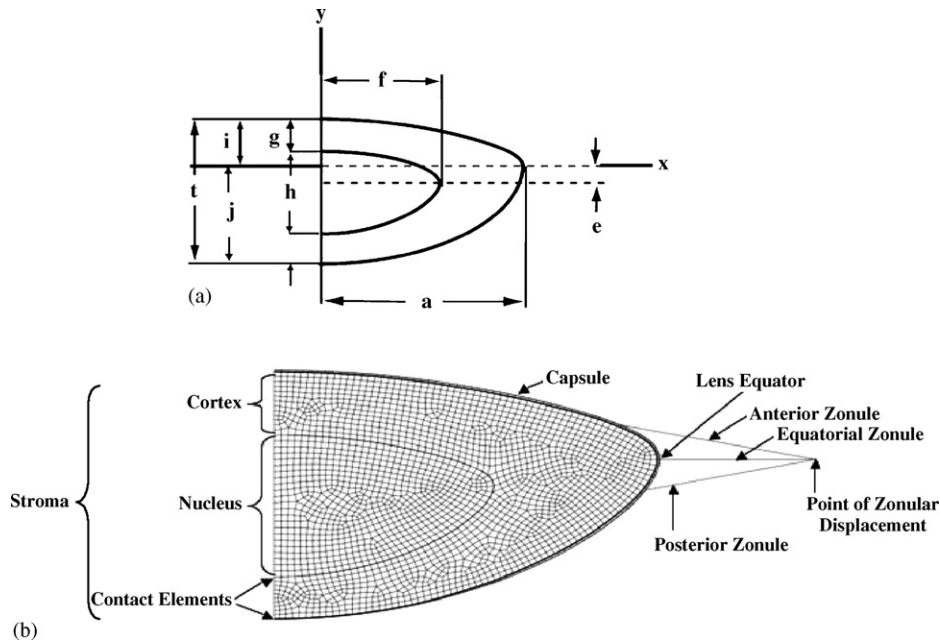


Fig. 1 – (a) Outline of the lens and lens nucleus. The xy -axis for Eq. (2.1) is shown. The dimensions for the outlines are given in Table 1. (b) FEM mesh of Profile I modeled with 2113 hybrid stromal and 118 capsular standard quadrilateral capsular elements. The position of the surface-to-surface contact elements are shown by the dark lines located at the capsular–cortical interface and the cortex–nucleus interface.

equations [27]:

$$\nu = \frac{3K - 2G}{6K + 2G} \quad (2.2)$$

$$E = \frac{9KG}{3K + G} \quad (2.3)$$

From Eq. (2.2), $\nu \cong 0.49999999$, indicating that the lens is negligibly compressible. From Eq. (2.3), the elastic modulus E , for both the cortex and nucleus is 150 Pa. The magnitude of this elastic modulus is consistent with that determined for endothelial cells, where $E = 130$ Pa [28].

2.2.2. Lens capsule and zonules

The baseline material properties of the lens capsule and zonules were obtained from the literature, Table 2. For the capsule, the Poisson's ratio was $\nu = 0.47$ [29], and the modulus of elasticity of the entire stroma, cortex, nucleus, anterior and posterior capsules, was $E_{\text{stroma}} = 1.7 \text{ E-4 MPa}$, $E_{\text{cortex}} = 1.7 \text{ E-4 MPa}$, $E_{\text{nucleus}} = 2.0 \text{ E-4 MPa}$, $E_{\text{anterior}} = 1.5 \text{ MPa}$, $E_{\text{posterior}} = 0.5 \text{ MPa}$, respectively [20,21]. The elastic modulus of the zonules was $E_{\text{zonules}} = 1.5 \text{ MPa}$ [30].

2.3. FEM

ABAQUS was used to analyze the axisymmetric discrete FEM model of the lens [31]. Standard constitutive equations for a two-dimensional axisymmetric problem were used with a mixed formulation based on displacement and pressure. The pressure variable was formulated with a Lagrange multiplier. This was done to accurately model the incompressibility of the lens and prevent the locking phenomenon. The bound-

ary condition was that all the nodes located along the y -axis were restrained from moving in the x direction but were free to move along the y -axis (Fig. 1a). The general discrete finite element formulation was used in which the axisymmetric solution of each element is approximated by a complete polynomial. The number of constants of the polynomial was equal to the degrees of freedom of each element. By having a completeness requirement, monotonic convergence of the elements was insured [9]. The nonlinear problem was solved by incrementally using a piecewise linear algorithm based on the Newton–Raphson procedure [9].

2.4. FEM mesh

Standard quadrilateral elements were employed to model the capsule [32–36]. Since the compressibility of the lens is negligible, with a bulk modulus much larger than its shear modulus, hybrid quadrilateral elements were used to model the lens cortex and nucleus. By using a mixed formulation these hybrid elements overcome the problems associated with modeling the nearly incompressible lens. Had a standard formulation been used for the lens stroma, the equilibrium equation could not be solved in terms of its displacement history because a purely hydrostatic pressure could be added without changing displacement. Conversely, a small change in displacement could induce a large increase in hydrostatic pressure [37].

The stress induced by pressure was treated as an independently interpolated basic solution variable. It was coupled to the displacement solution through a compatibility and constitutive relationship. Fig. 1(b) shows a typical converged mesh obtained after several trials with all three sets of zonules attached.

Table 2 – Sensitivity study: baseline, range and critical values

Material and geometric properties	Baseline	Minimum	Maximum	Critical value that reduces the response
Distance of the anterior zonular-capsule attachment from the lens equator (mm)	1.5	0.5	1.5	>0.5
Distance of the posterior zonular-capsule attachment from the lens equator (mm)	1.0	0.25	1.0	>0.25
Elastic modulus (MPa)				
Stroma	1.7E-04	0.5E-4	3.0E-1	>4.0E-4
Cortex	1.7E-4	0.5E-4	8.0E-4	>4.0E-4
Nucleus	1.9E-04	0.5E-4	8.0E-4	>4.0E-4
Anterior capsule	1.5	0.25	3	<0.75
Zonules	1.5	0.1	6	<0.5
Lens stroma Poisson's ratio	0.49999999	0.38	0.49999999	<0.499
Capsular thickness (μm)	24	5	50	<0.50
Intralenticular pressure (Pa)	0	67	670	No effect
Strength of the attachment between the cortex and nucleus				
Contact element stiffness (N/mm)	No contact elements	0.1	2	No effect
Contact element frictional coefficient	No contact elements	0.2	2	No effect
Strength of the attachment between the capsule and cortex				
Contact element stiffness (N/mm)	No contact elements	0.1	1	>0.1
Contact element frictional coefficient	No contact elements	0.0025	0.2	>0.01

2.5. FEM convergence

Since the monotonic convergence of the nonlinear finite element solution is problem dependent, and not guaranteed, the converged solution was obtained using an energy-based convergence criterion. The difference between the external virtual work done and the internal virtual strain energy [9,10] was calculated at each incremental iteration. The results were then compared to those at the previous iteration and checked against a specified tolerance. The final converged solution was obtained by coupling this criteria with H and P convergence, in which the number of mesh elements, and the degree of the polynomial used in the element displacement function were respectively increased. The 2113 stromal and 118 capsular element mesh was identified as the converged mesh (Fig. 2a).

2.6. Application of zonular traction to baseline lens

Although multiple anatomical studies have demonstrated variation in zonular insertion into the equatorial region of the capsule, the anterior, equatorial and posterior zonules predominate. Moreover, it has been demonstrated that a simplified zonular model is sufficient for modeling lenticular accommodation [14].

In this model, zonular traction (ZT) was applied to the lens capsule by differing anatomic groups of zonules. The ZT was exerted by: (1) the equatorial zonules alone or (2) the anterior and posterior zonules together or (3) all three sets of zonules simultaneously. The equatorial zonules insert directly into the lens equator. The anterior and posterior zonules insert into the lens capsule, 1.5 and 1.0mm central to the edge of the lens equator on their corresponding surface of the lens. At baseline, no external traction was applied to the zonules. ZT was applied at the point where the zonules meet and within the

lenticular equatorial plane (Fig. 1b). In this study, displacement of the lens equator or zonular displacement is the independent variable used to assess changes in central optical power (COP). Neither the ciliary body nor the ciliary muscle was modeled in this analysis.

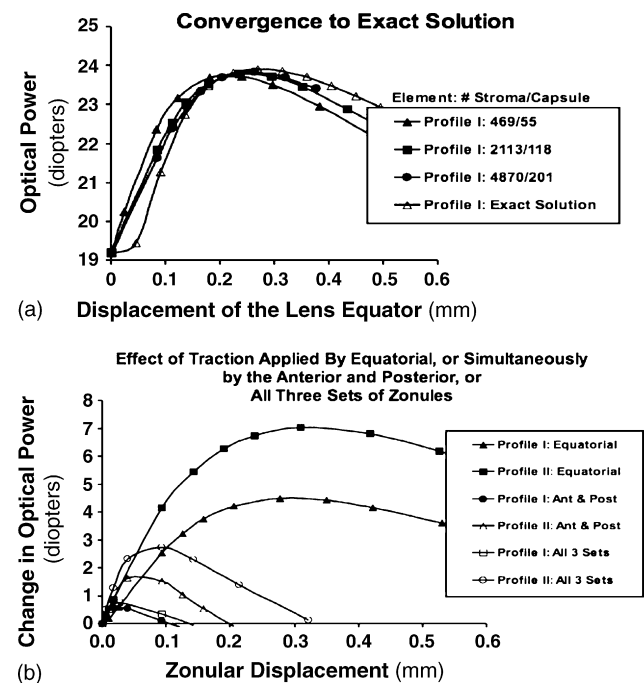


Fig. 2 – (a) Convergence of the FEM analysis to an exact solution [39] of the change in central optical power in response to equatorial zonular traction. (b) The change in central optical power associated with traction applied by only the equatorial, or by the anterior and posterior together, or by all three sets of zonules simultaneously.

3. Parametric study

3.1. Parametric variables

This parametric study evaluated the effect of geometric and force related variables on the change in central optical power (COP) of the lens by varying one variable at a time, from low to high, while keeping the other variables at their baseline values, Table 2. Each of the following parameters was independently evaluated: capsular thickness; stiffness of the capsule; stiffness of the entire lens stroma, its cortex, nucleus, and zonules; Poisson's ratio of the stroma; strength of the capsular-cortical and cortical-nuclear attachments; intralenticular pressure; and the location of attachment of the anterior and posterior zonules to the lens, Table 2. To determine the effect of baseline lens shape, on COP, the response of the five lens profiles were compared. Profile I was used for the sensitivity study because it gave the median increase in central optical power in response to equatorial ZT.

Since the central posterior capsular thickness does not change thickness with aging [20,21], its thickness was held constant. Values were assigned for the thickness of the anterior capsule, Table 2. The balance of the capsule, except for this central posterior portion, was proportionally adjusted in thickness.

The actual strength of the attachments of the capsule to the cortex and the cortex to the nucleus is unknown. In order to assess the impact of adhesion at these interfaces, the strength of the attachments was varied and evaluated. To allow the surfaces to move apart and slide relative to each other, surface-to-surface contact elements, with a range of frictional coefficients and stiffness, were placed between these interfaces. To simulate the condition when the surfaces are fused together, contact elements were omitted.

3.2. Central optical power (COP) [12]

$$\text{COP} = \frac{n_1 - n_a}{r_a} + \frac{n_1 - n_a}{r_p} - \frac{t(n_1 - n_a)^2}{r_a r_p n_1} \quad (3.1)$$

where $n_1 = 1.42$ [38], $n_a = 1.336$ and $t = \text{CLT}$.

The anterior, r_a and posterior, r_p radii of curvatures are calculated by using the radii of the sphere that fits the central 1.6 mm diameter aperture of each lenticular surface before and after zonular traction is applied [12].

3.3. Force

The total force required for ZT was determined.

3.4. Idealized lens

Baseline lens shape appears to be a major determinant of the response of COP to ZT [39]. Since none of the studied lenses demonstrated changes in COP comparable to the young *in vivo* human lens, an idealized lens was modeled. For this lens, central radii of curvatures, 11.7 mm for the anterior surface and of 7.7 mm for the posterior surface, were assigned. Using these curvatures, an equatorial radius of 4.3 mm, and central

anterior stromal thicknesses of 1.9 mm, the coefficients for Eq. (2.1) were calculated to obtain the idealized lens profile, Table 1.

Based on these sensitivity studies, the assigned elastic moduli for the cortex, nucleus, anterior and posterior capsules, and zonules of the idealized lens were 170 Pa, 220 Pa, 0.5 MPa, 1.5 MPa, and 1.5 MPa, respectively. The central thicknesses of the anterior and posterior capsules were 24 and 5 μm , respectively. Surface-to-surface contact elements with a stiffness of 0.1N/mm and a frictional coefficient of 0.005 were placed between the capsule and cortex to simulate the weak attachment of the capsule to the cortex.

4. Results

4.1. Validation

The accuracy of the developed model was validated because the results of the converged FEM mesh approached the exact solution that was obtained independently from the solution of two-second order, nonlinear differential equations governing the behavior of Profile I in response to ZT applied by only the equatorial zonules [39] (Fig. 2a).

4.2. Change in central optical power (COP)

Commencing at zero tension, increasing ZT always increased COP (Figs. 2b and 3a). This was true for every lens, including Profiles II [17] and V [19] which were reported to be in

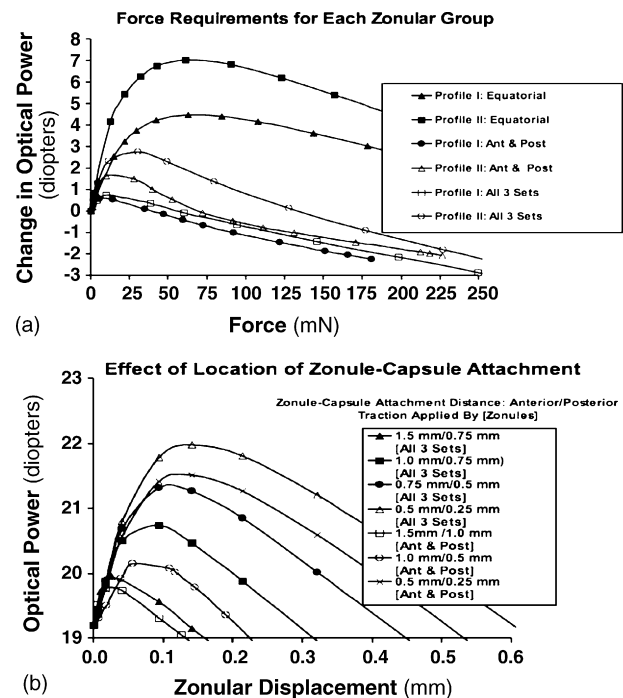


Fig. 3 – (a) The force required to change the central optical power when zonular traction is applied by only the equatorial, or by the anterior and posterior, or all three sets of zonules. (b) The effect of the distance from the lens equator of the anterior and posterior zonular capsular attachments.

the accommodated state, whether the ZT was applied to the equatorial zonules alone, to the anterior and posterior zonules together, or to all three sets of zonules simultaneously (Figs. 2b and 3a). With minimal ZT, the COP increased from its baseline to reach its positive maximum power. The model predicts that with further force, there was always a reversal in the direction of change and a diminution in COP (Fig. 3a).

Simultaneous traction on the anterior and posterior zonules for all locations of their attachments to the lens capsule was associated with an increased COP (Fig. 3b). Moreover, the closer these zonular attachments approached the lens equator, the greater the magnitude of the increase in COP. These effects occurred independent of the change in material and geometric properties of the lens. Whether zonular traction was applied by the equatorial zonules, or simultaneously by the anterior and posterior zonules, or by all three sets of zonules, a variation in a specific geometrical or material property had a similar effect on the change in COP.

4.3. Baseline shape

Baseline shape of the lens affected the change in COP associated with equatorial ZT (Fig. 4a).

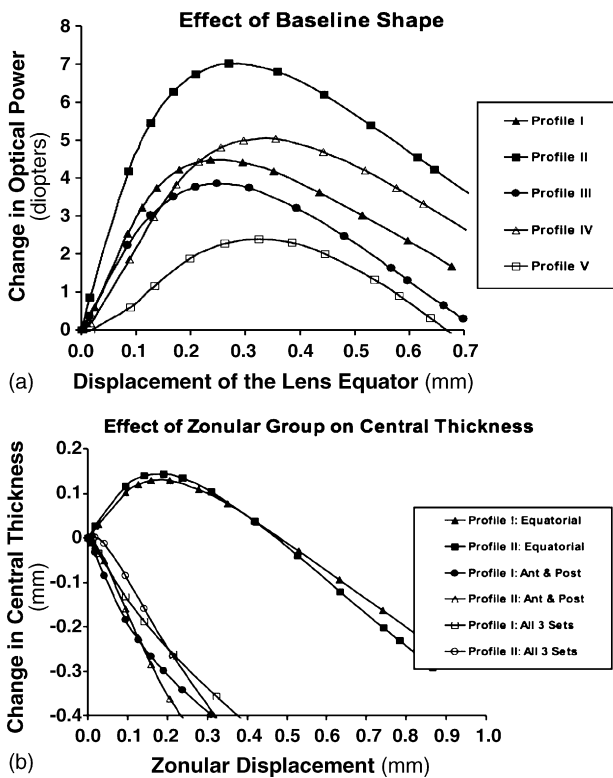


Fig. 4 – (a) Effect of baseline shape on the change in central optical power in response to equatorial zonular traction. (b) Effect of the change in central lens thickness when zonular traction is exerted by the equatorial zonules only, the anterior and posterior zonules together, or all three sets of zonules simultaneously.

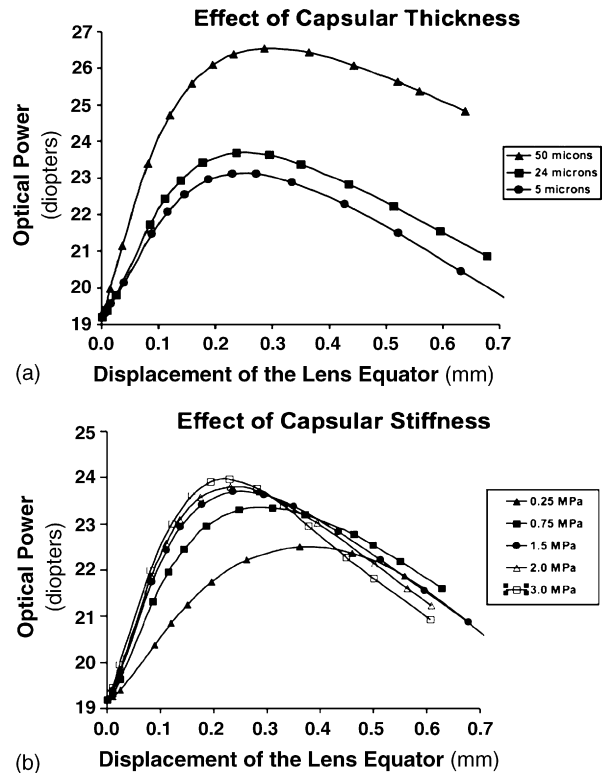


Fig. 5 – The effect of (a) capsular thickness and (b) capsular stiffness on the change in central optical power associated with equatorial zonular traction.

4.4. Change in central lenticular thickness (CLT)

When tension to the equatorial zonules was applied from the zero baseline, CLT increased to a maximum and then decreased with further ZT. However, when ZT was applied, to the anterior and posterior zonules, or all three sets of zonules simultaneously, CLT immediately decreased (Fig. 4b).

4.5. Baseline capsule thickness

With equatorial ZT, the thicker the capsule, the greater the COP increased (Fig. 5a).

4.6. Material properties

Increasing capsular stiffness increased the COP. This effect was most apparent for capsular stiffness >0.75 MPa after which COP approaches the maximum response to increasing capsular stiffness (Fig. 5b). Decreasing the stiffness of the entire lens stroma, its cortex, or nucleus was associated with an increase in COP (Fig. 6a-c).

For all values of Poisson's ratio, $0.38 \leq \nu \leq 0.49999999$, equatorial ZT, commencing at zero, increased COP. The COP approached a maximum for $\nu > 0.499$ (Fig. 6d), Table 2.

For zonular stiffness <0.5 MPa, the change in COP is significantly reduced in response to equatorial ZT (Fig. 7a).

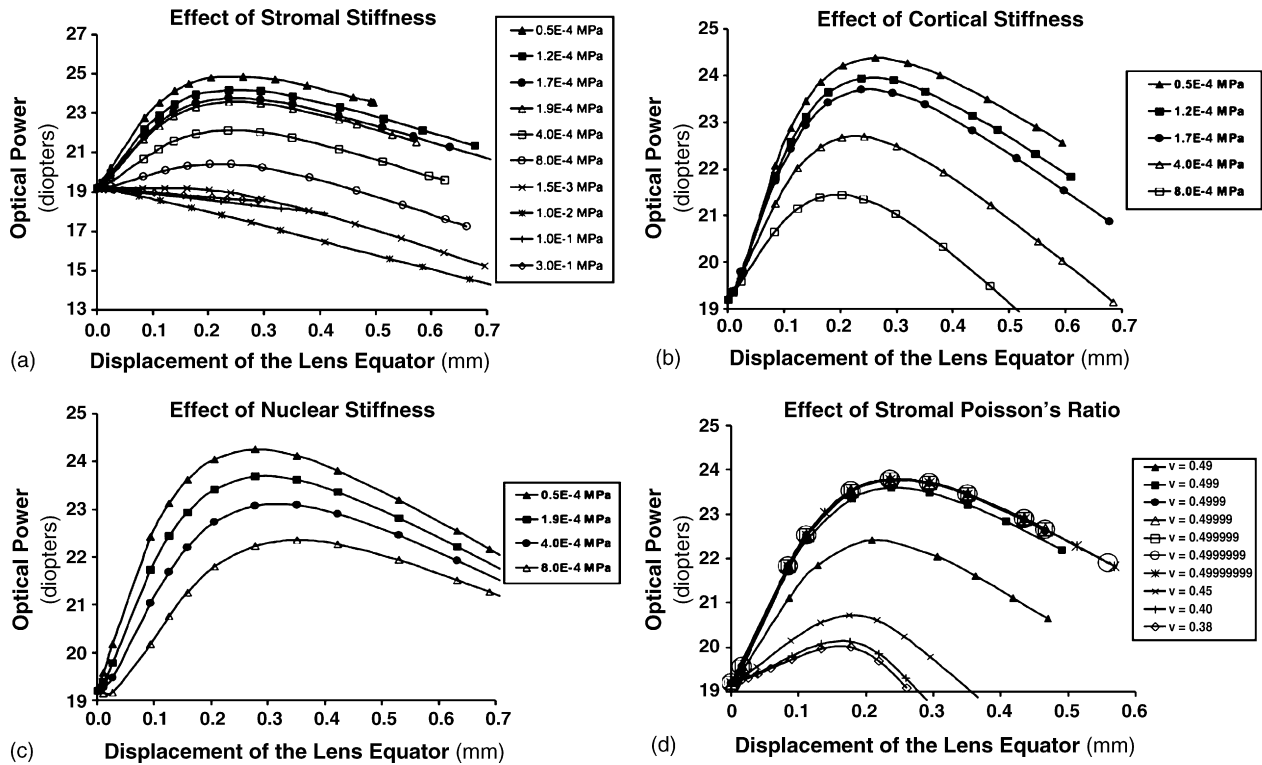


Fig. 6 – Effect of the elastic modulus of the (a) stroma (b) cortex (c) nucleus and (d) Poisson's ratio on the change in central optical power associated with equatorial zonular traction.

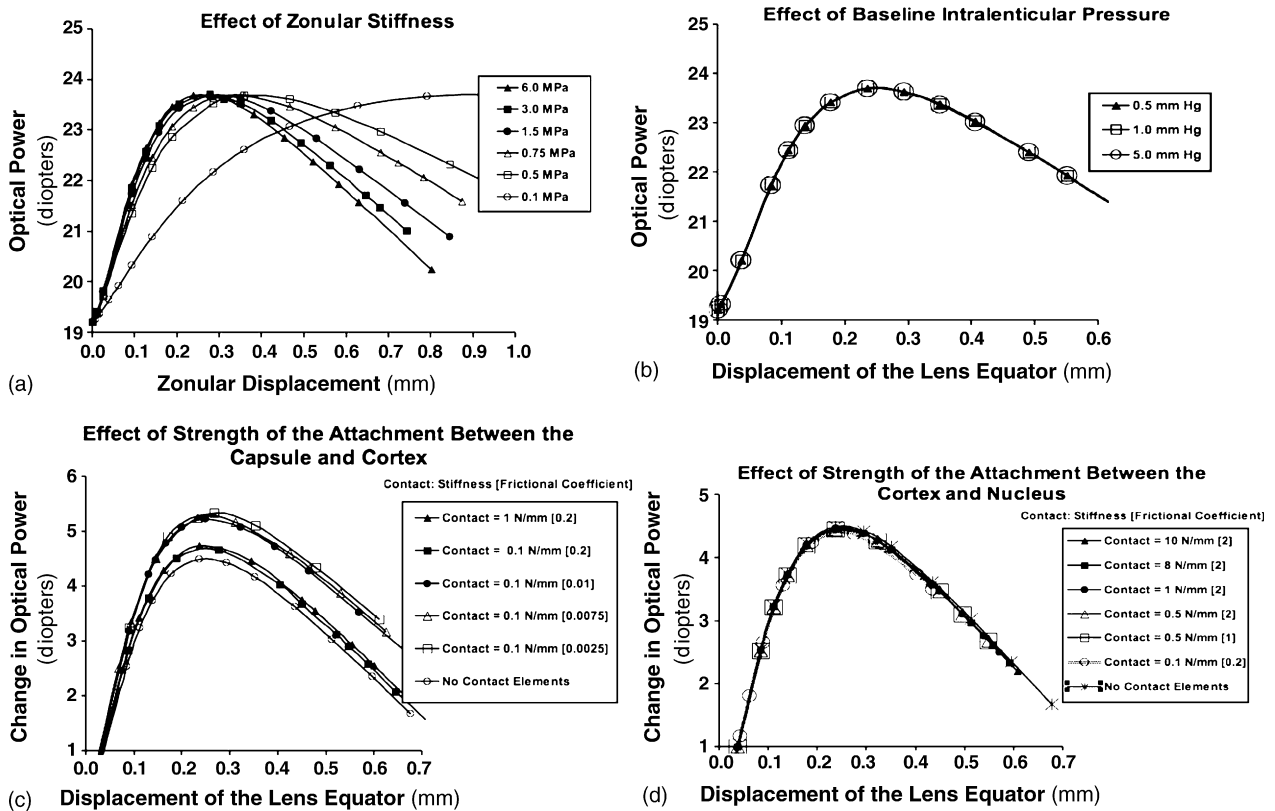


Fig. 7 – The effect of (a) zonular stiffness (b) baseline intralenticular pressure and the strength of the attachments between the (c) capsule and cortex and (d) cortex and nucleus on the change in central optical power associated with equatorial zonular traction.

4.7. Baseline intralenticular pressure

Baseline intralenticular pressure, between 0.1 and 5 mm Hg, did not appear to affect the change in COP associated with equatorial ZT (Fig. 7b), Table 2. This is consistent with the intralenticular pressure of freshly preserved post-mortem intact human lenses of <1 mm Hg measured in our laboratory.

4.8. Strength of the cortical/nuclear and capsular/cortical attachments

The FEM predicted that a weak attachment between the capsule and cortex increases the response, which infers that the capsule is not firmly bound to the cortex (Fig. 7c). The strength of the attachment between the nucleus and cortex did not appear to have an effect on the change in COP in response to equatorial ZT (Fig. 7d), Table 2.

4.9. Idealized lens

The COP of the idealized lens increased 10 diopters in response to 15 mN of equatorial ZT (Fig. 8a). Both the central anterior and posterior surfaces steepened and moved outward, while their peripheral surfaces flattened with equatorial ZT (Fig. 8b). The outward movement of the central posterior sur-

faces accounted for approximately 1/3 of the increase in CLT (Fig. 8c).

5. Discussion

5.1. Accuracy

The accuracy of our FEM was assessed by comparing the outcomes of the idealized lens to the actual changes in COP and lens shape that occur *in vivo*. The idealized lens satisfied all of the anatomic and physiological constraints of the human eye.

5.1.1. Lens compressibility and accommodation

It has been demonstrated that when pressures greater than 101 kPa are applied in incremental steps of 20 kPa to the lens, it responds synergetically in a linear fashion [40]. Since normal intraocular pressure is 2.6 kPa, and the change in intralenticular pressure during accommodation is approximately 1.3 kPa, it is unlikely that the compressibility of the lens changes during normal accommodation [41].

5.1.2. Strength of the cortical/nuclear and capsular/cortical attachments

The FEM model demonstrates that a weak attachment between the capsule and the cortex enhances the effect of

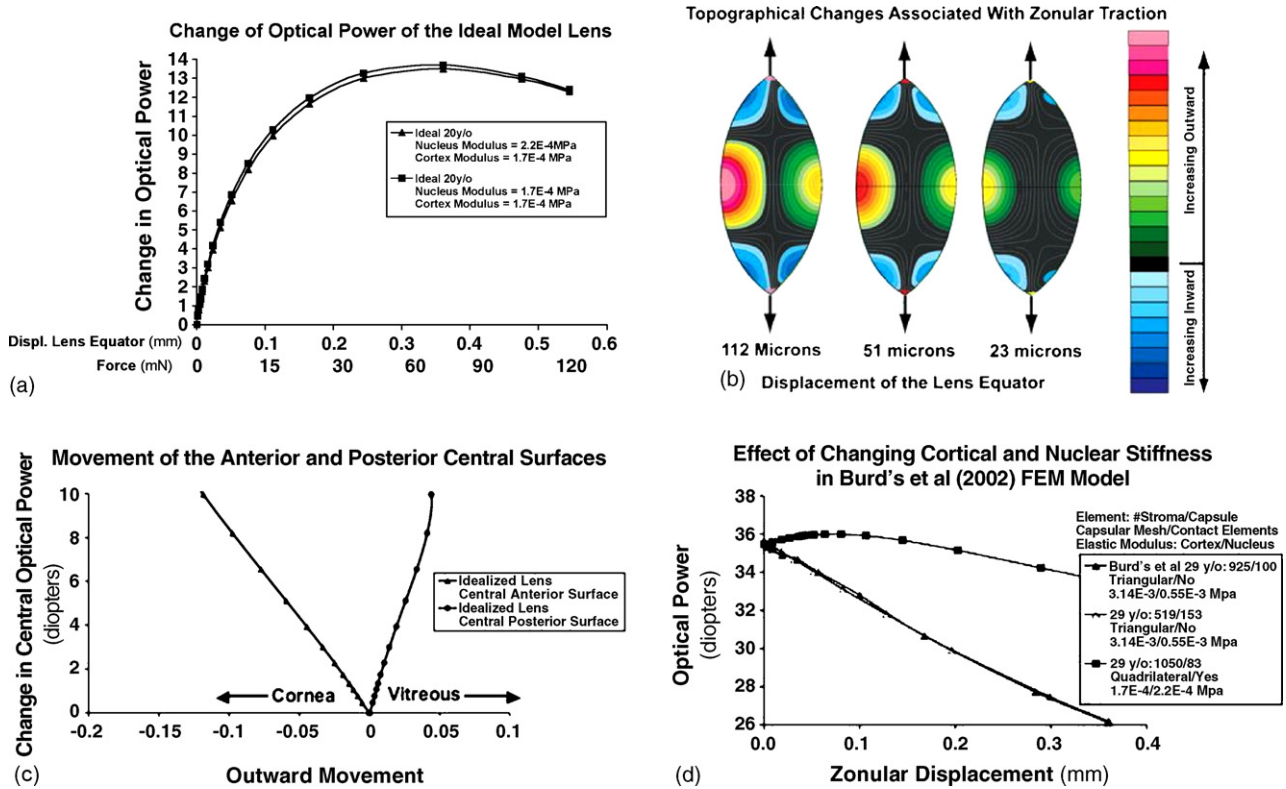


Fig. 8 – For equatorial zonular traction applied to the idealized lens the following are evaluated: (a) the force and displacement required to change the central optical power, (b) the topographical changes, and (c) the movement of the central anterior and posterior surfaces. (d) We duplicate Burd's et al [12] results for the 29y/o lens. Then we change the elastic moduli of the cortex and nucleus to 1.7 MPa and 2.2 E-4 MPa, respectively, replace the capsular triangular mesh elements with standard quadrilateral elements, add surface-to-surface contact elements between the capsule and cortex, and converge the solution.

ZT on COP. Consistent with this finding, there is no cement substance or other extracellular material between the capsule and cortical cells, and there are few interlocking processes between the first eight to ten layers of cortical cells that are under the capsule [42]. Moreover, the cortical lens fibers are easily hydro-dissected from the lens capsule [43,44]. Consequently, surface-to-surface contact elements should be included in FEM modeling of the capsule–cortical interface to simulate its weak adhesion. The strength of the attachment between the cortex and nucleus has no effect on the COP in response to equatorial ZT.

5.1.3. Constraints of human lenticular accommodation

The following anatomical, physiological, and topographical constraints were employed to confirm that the model represented human lenticular accommodation:

1. The change in the equatorial radius of the lens model must be less than the maximum 1.3 mm space between the lens equator and the ciliary sulcus [45]. Any change greater than this would extend the equator of the lens beyond the physical limits of the eye.
2. The total force required to induce a large change in central lenticular optical power must be less than the maximum force capacity of the ciliary muscle. An upper estimate for the maximum force capacity of the human ciliary muscle is 50 mN. This was based on the following two sources. The maximum force capacity of the human ciliary muscle, estimated from the deformation of the surfaces of spinning human lenses, is 16 mN [46]. The maximum force exerted by a 6 mm wide strip of monkey ciliary muscle in response to pilocarpine is 3.2 mN [47]; i.e., the load plus the force of contraction (Tables 1 and 2 of this reference). Since the circumference of the monkey ciliary ring is approximately 48 mm the total force capacity of the monkey ciliary muscle is approximately 26 mN.
3. The lens model must simulate the well-documented and non-controversial shape changes that the crystalline lens undergoes during *in vivo* human accommodation. These are an increase in central thickness [48–50], steepening of its anterior central surface, flattening of its anterior peripheral surface [50–54], and a large increase in central optical power [2,3] in response to an alteration in zonular tension.

5.1.4. Increase in central optical power

Although the human lens has a varying index of refraction (GRIN), COP of the modeled lenses was calculated using a fixed refractive index. This approximation minimally alters the validity of using Eq. (3.1) to calculate COP [55]. In addition, the central refractive index of the lens does not appear to change significantly with age [38].

Zonular traction, when applied to the idealized lens induced a 10-diopter increase in COP as a consequence of a decrease in the central radii of curvatures of its anterior and posterior surfaces from 11.7 to 7.1 mm and from 7.7 mm to 5.0 mm, respectively. Korte et al. [49] has reported that during *in vivo* human accommodation of 10 diopters, a similar decrease in the central anterior and posterior surface radii of curvature from 11.7 to 7.6, and from 7.6 to 5.4 mm, respectively occur.

5.1.5. Increase in CLT

Using an A-scan probe designed to track the eye [56] and partial coherence tomography [57], it has been demonstrated that during human accommodation, *in vivo*, CLT increases with the outward movement of the central posterior surface accounting for $\sim 1/3$ of the total CLT increase (Fig. 8c). Continuous A-scan ultrasonography during dynamic primate *in vivo* accommodation [58] demonstrates a similar graphic relationship between COP and the relative movement of the anterior and posterior lenticular surfaces as predicted by the FEM. These independent experimental findings, using high-resolution techniques *in vivo*, are strong evidence for the validity of the FEM predictions.

5.1.6. Central anterior surfaces steepen and peripheral surfaces flatten

Increasing ZT, from the zero baseline, induces central anterior surface steepening and peripheral flattening (Fig. 8b). These curvature changes have been observed *in vitro* when ZT is applied to human lenses [59–61], and have been documented during *in vivo* accommodation by: examining the reflections from the anterior lenticular surface [52,53], Scheimpflug photography [50], optical coherence tomography [54], and aberrometry [51,62–64]. None of these *in vivo* studies assessed the amount and pattern of zonular tension.

5.1.7. Force capacity of the ciliary muscle and the equatorial circumlental space

In the idealized lens model, when zonular tension reached 15 mN, the displacement of the lens equator increased by 112 μm , and the central optical power increased by 10 diopters. The magnitude of the force and the displacement required to obtain this increase in central optical power are within the anatomical constraints of the circumlenticular equatorial space and the physiological force capacity of the ciliary muscle.

From this accommodated state, the optical power of the lens can be reduced in two alternate ways (Figs. 4a and 8a). One is to reduce the zonular tension to permit reduction in COP, a mechanism suggested by Schachar [65–67]. The reduction in force and lens equatorial diameter associated with this alternative insures that the decrease in COP occurs within the anatomical and force constraints of the human eye.

Alternatively, the COP of the lens can be reduced, by increasing zonular tension. Under this option, the FEM model predicts that to decrease the COP of the lens from its maximally accommodated state, a mechanism proposed by Helmholtz [48], a 4 mm increase in the equatorial diameter of the lens and a force of more than 300 mN would be required. This is anatomically and physiologically impossible. Consequently, the model indicates that relaxation of zonular tension is the only alternative for reducing the COP of the lens from its maximally accommodated state.

5.2. Direction of movement of the lens equator

The FEM predicts that the positional change of the lens equator associated with a 10-diopter increase in COP is approximately 112 μm or $<3\%$ of the equatorial radius of the lens. This small displacement is below the resolution of the MRI used

to acquire images of the human lens. As a consequence, MRI images of human eyes that have been carefully registered did not demonstrate statistically significant movement of the lens equator during *in vivo* accommodation [68]. Likewise, when high-resolution, *in vivo*, ultrasound biomicroscopic images of primate [69,70] and human [71] eyes were registered, the equator of the lens moved less than 100 μm outward toward the sclera during the accommodative process.

There are many studies, contrary to the predictions of this FEM that demonstrate a large decrease in lens equatorial diameter during accommodation [19,53,72–75]. None of these experiments included positional references, coincident image registration, triangulation, and eye tracking to control for spurious movements of the eye between collection of the images [61,70,76–83].

Since the FEM suggests that lenticular accommodation is a small displacement phenomenon, these controls are essential to differentiate intraocular lens movements from confounding extraocular movements. Statistical methods employed in some studies to control for extraocular movements are not reliable since the convergent and excyclotorsion movements of the eyes are not random.

5.3. Mechanism of accommodation

During maximum *in vivo* accommodation the anterior and posterior zonules relax to the point of curling [84–86]. Since the lens is stable during accommodation [87–89], and the anterior and posterior zonules are relaxed, it appears from the FEM model that the equatorial zonules are the active components of accommodation. Other FEM analyses [90,91] and a more precise differential equation model [39] also conclude that ZT applied by the equatorial zonules induces lenticular accommodation.

The appearance and level of tension on the equatorial zonules during human *in vivo* accommodation is unknown. The equatorial zonules are not visible with slit lamp photography because of their small diameter. The path of the equatorial zonules has only been established by scanning electron microscopy [14,92,93] and recently *in vivo* with ultrasound biomicroscopy [14]. The equatorial zonules, which are less than 1 mm in length, extend from the valleys between the ciliary processes to the lens equator. Ludwig's et al. [86] specifically excluded the equatorial zonules from their ultrasound biomicroscopic study because, as described in their methodology, only zonules that were at least 1 mm long were analyzed.

The results of other FEM models differ from our analysis [12–15]. These studies concluded that the equatorial diameter of the lens decreases during accommodation. The difference in outcome may relate to their use of a discontinuous function for the lens profile; consisting of a fifth order polynomial, a straight line, and a circular end cap. Also, in these models triangular elements were used to model the capsule and surface-to-surface contact elements were not placed between the capsule and cortex.

Importantly, in all of these studies the cortex of a 29y/o_{acc} lens was asserted to be six times harder than its nucleus [12–15]. Recently these material properties of the lens cortex and nucleus, were re-evaluated and found to be incorrect [94]. This conclusion is supported by *in vitro* measurements of *fresh*

human lenses using Brillouin light scattering, a non-invasive technique [23], penetration [43], and routine clinical observation during cataract extraction by phacoemulsification [95], all of which demonstrate that the hardness of the lens nucleus is either the same or greater than its cortex.

We were able to duplicate Burd's et al [12] analysis of the 29y/o_{acc} lens when employing their same moduli, and a coarse unconverged mesh with identical type of elements (Fig. 8d). However, by employing standard quadrilateral elements to model the capsule, suitable elastic moduli for the cortex and nucleus, and surface-to-surface contact elements placed between the capsule and cortex in their geometric model, we demonstrate, that beginning at zero, ZT increases COP when a converged solution is used (Fig. 8d). In addition, we find that under this scenario ZT only minimally changed COP.

5.4. Etiology of presbyopia

Our FEM model predicts that increasing capsular stiffness and/or thickness increases COP induced by ZT making it unlikely that the known age-related increase in capsular stiffness and thickness [20,21] are the etiologic causes of presbyopia.

The model predicts that increasing the hardness of the entire stroma, cortex, or nucleus decreases the COP induced by ZT. However, there does not appear to be consistent change in cortical, nuclear or stromal hardness of fresh human lenses <40y/o *in vitro* [43] or *in vivo* [24] when most of the accommodative amplitude is lost. There are no optical changes in the lens that suggest nuclear sclerosis of human lenses in eyes <40y/o *in vivo* [96]. Even following 2 weeks of storage in liquid nitrogen, pieces of lenses aged 14–25 years [26,97] do not demonstrate a significant change in stiffness [26,97,98].

To further assess the effect of lens hardness on accommodation, the elastic modulus of the entire lens stroma, cortex and nucleus of the idealized lens was varied from 150 Pa to 7.5 kPa. As predicted by the parametric study, increasing the elastic modulus of the lens decreased the maximum COP associated with equatorial ZT (Fig. 9a). In addition, with an increase in lens stiffness, the mean efficiency of ZT, change in central optical power per micron of displacement of the lens equator between 0 and 112 μm decreases (Fig. 9b).

Accordingly, if lens hardness was the etiology of the decline in accommodative amplitude with age, a younger lens should change shape faster than an older lens for all accommodative demands. Careful evaluation of the dynamics of accommodation has demonstrated that in the linear range of accommodation there is no statistical significant difference in the time constant or the peak/velocity/amplitude of subjects aged 16–40 years [99–102]. This finding, and the lack of change in lens stromal hardness in the young lens, makes it unlikely that the normal physiological change in hardness of the cortex, nucleus or entire lens stroma is the etiology of the 10-diopter decline in accommodative amplitude that occurs from birth to 40y/o [2,3].

The FEM predicts that zonular stiffness would have to decrease by a factor of three to reduce the COP response to equatorial ZT. Since it has been demonstrated that the zonules become stiffer with age [103], it is unlikely that a change in

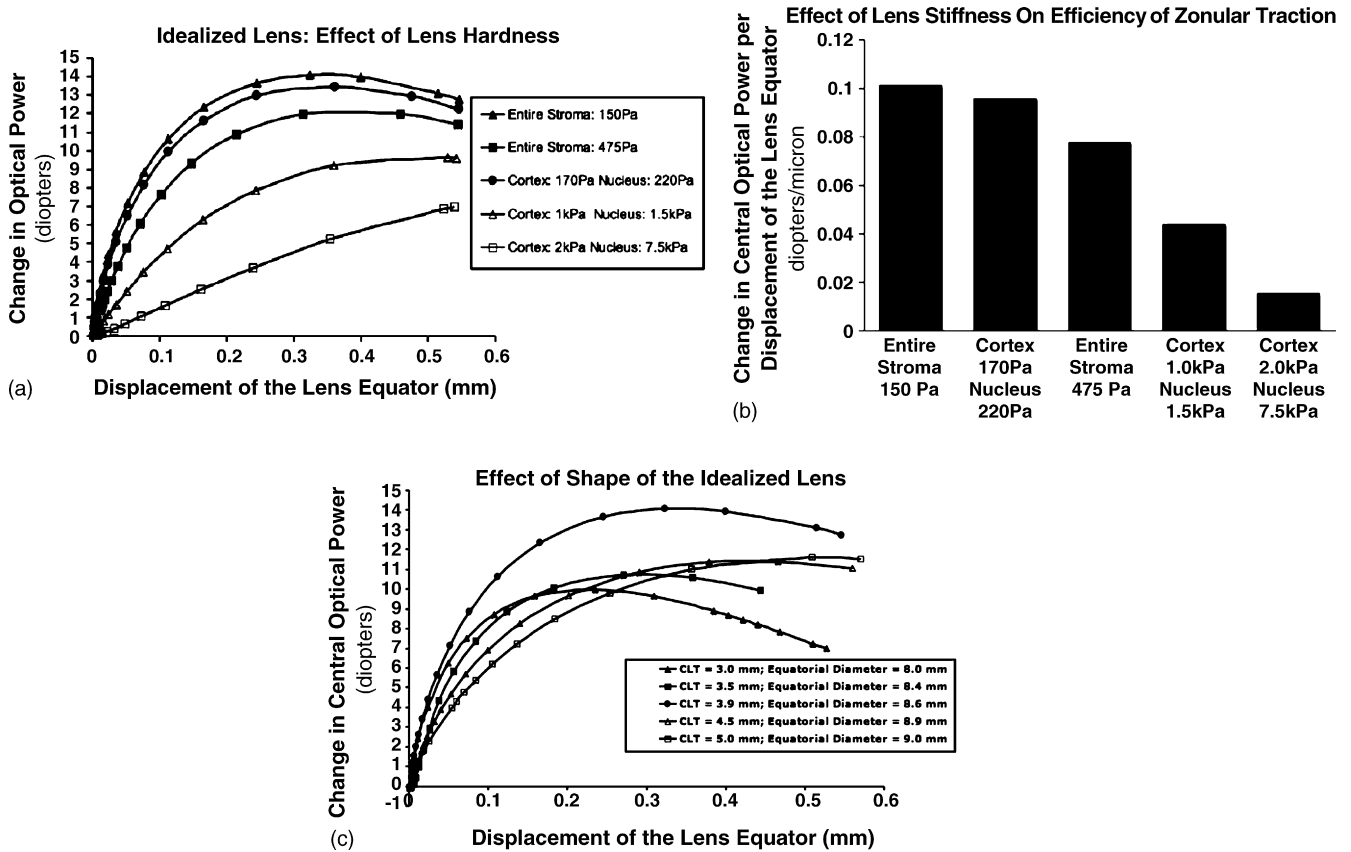


Fig. 9 – Effect of stiffness of the entire stroma, cortex, and nucleus of the idealized lens on (a) the change in central optical power and (b) the mean efficiency of equatorial zonular traction, diopters of increase in central optical power for each micron of peripheral displacement of the lens equator from 0 to 112 μm . (c) The effect of changing the thickness and equatorial diameter of the idealized lens on the response of its central optical power to equatorial zonular traction.

zonular stiffness would account for the age-related decline in accommodative amplitude.

This study demonstrates that the change in COP associated with equatorial ZT depends on lens shape. It is possible that the age-related change in lens shape is the etiology of presbyopia. Between 20 and 40y/o the lens increases in thickness [104] and equatorial diameter [105,106] with a small change in central [104] and a non-significant change in peripheral, inferred from aberrometry [107,108], curvatures. To simulate these changes, the thickness and equatorial diameter of the idealized lens were altered by moving the anterior and posterior surfaces without changing their curvatures. When the thickness and equatorial diameter of the idealized lens is decreased or increased, the maximum COP associated with equatorial ZT declines (Fig. 9c). Therefore it is unlikely that the normal change in lens shape is the etiology of presbyopia.

An alternate possibility for the etiology of presbyopia is an age-related decline in maximum force applied by the zonules. The equatorial diameter of the lens increases throughout life as a consequence of the continuous mitosis of its stem cells [105]. This predictable and progressive increase in the equatorial diameter of the lens will cause a reduction in the distance between the lens and ciliary body, thereby reducing the tension on the zonules supporting the lens. As zonular tension is reduced, the model predicts that COP decreases. The

physiologic age-related decline in the amplitude of accommodation [2,3], referred to as presbyopia, could be the functional manifestations of this normal equatorial lens growth.

6. Conclusion

This sensitivity study, using nonlinear FEM analysis, demonstrated that ZT from zero increased COP. This increase in COP occurred over a large range of Poisson's ratios. ZT tension applied by only the equatorial zonules alone satisfied the constraints of the force capacity of the ciliary muscle, the limitations of the equatorial circumlental space, and the topographical lenticular changes that occur during human accommodation.

Increasing capsular stiffness or its thickness increased the magnitude of the change in COP of the lens associated with a fixed ZT. Weakening the attachment between the capsule and its underlying cortex increased the magnitude of the change in COP. Increasing the elastic modulus of the entire lens stroma, cortex, or nucleus decreased the maximum change in COP. Decreasing the amount of ZT, while holding the elastic moduli of the lens fixed, decreases the maximum change in COP. Since the elastic moduli of the lens do not change significantly in young eyes, it is unlikely to be the etiology

of the progressive decline of accommodative amplitude seen throughout life. Normal equatorial lens growth can explain the progressive decrease in the maximum ZT that results in the age-related decline in accommodative amplitude.

REFERENCES

- [1] B.K. Pierscionek, R.A. Weale, Presbyopia—a maverick of human aging, *Arch. Gerontol. Geriatr.* 20 (3) (1995) 229–240, Medline.
- [2] F.C. Donders, On the Anomalies of Accommodation and Refraction of the Eye, The Sydenham Society, London, UK, 1864.
- [3] A. Duane, Textbook of Ophthalmology, 5th ed., J.B. Lippincott Company, Philadelphia, PA, 1917.
- [4] E.Y. Ng, E.H. Ooi, FEM simulation of the eye structure with bioheat analysis, *Comput. Meth. Prog. Biomed.* 82 (3) (2006) 268–276.
- [5] J.T. Cheung, M. Zhang, A.K. Leung, Y.B. Fan, Three-dimensional finite element analysis of the foot during standing—a material sensitivity study, *J. Biomech.* 38 (5) (2005) 1045–1054, doi:10.1016/j.jbiomech.2004.05.035.
- [6] M. Lengsfeld, J. Kaminsky, B. Merz, R.P. Franke, Sensitivity of femoral strain pattern analyses to resultant and muscle forces at the hip joint, *Med. Eng. Phys.* 18 (1) (1998) 70–78, doi:10.1016/1350-4533(95)00033-X.
- [7] R.A. Baldewsing, C.L. de Korte, J.A. Schaar, F. Mastik, A.F. van der Steen, Finite element modeling and intravascular ultrasound elastography of vulnerable plaques: parameter variation, *Ultrasonics* 42 (1–9) (2004) 723–729, doi:10.1016/j.ultras.2003.11.017.
- [8] O.C. Zienkiewicz, The Finite Element Method, vol. 2, 4th ed., McCraw Hill, London, UK, 1989.
- [9] K.-J. Bathe, Finite Element Procedure, Prentice Hall, Englewood Cliffs, NJ, 1996.
- [10] R.D. Cook, D.S. Malkus, M.E. Plesha, R.J. Witt, Concepts and Applications of Finite Element Analysis, 4th ed., Wiley, NY, 2002.
- [11] H.J. Burd, S.J. Judge, M.J. Flavell, Mechanics of accommodation of the human eye, *Vis. Res.* 39 (9) (1999) 1591–1595, doi:10.1016/S0042-6989(98)00298-3.
- [12] H.J. Burd, S.J. Judge, J.A. Cross, Numerical modelling of the accommodating lens, *Vis. Res.* 42 (18) (2002) 2235–2251, doi:10.1016/S0042-6989(02)00094-9.
- [13] H. Martin, R. Guthoff, T. Terwee, K.P. Schmitz, Comparison of the accommodation theories of Coleman and of Helmholtz by finite element simulations, *Vis. Res.* 45 (22) (2005) 2910–2915, doi:10.1016/j.visres.2005.05.030.
- [14] O. Stachs, H. Martin, D. Behrend, K.P. Schmitz, R. Guthoff, Three-dimensional ultrasound biomicroscopy, environmental and conventional scanning electron microscopy investigations of the human zonula ciliaris for numerical modelling of accommodation, *Graefes. Arch. Clin. Exp. Ophthalmol.* 244 (7) (2006) 836–844.
- [15] E.A. Hermans, M. Dubbelman, G.L. van der Heijde, R.M. Heethaar, Estimating the external force acting on the human eye lens during accommodation by finite element modelling, *Vis. Res.* 46 (21) (2006) 3642–3650.
- [16] C.H. Chien, T. Huang, R.A. Schachar, A mathematical expression for the human crystalline lens, *Comp. Ther.* 29 (4) (2003) 245–258, Medline.
- [17] R.R. Krueger, Retinal imaging aberrometry, author reply, *Ophthalmology* 109 (3) (2002) 406–407.
- [18] M.J. Lizak, M.B. Datiles, A.H. Aletras, P.F. Kador, R.S. Balaban, MRI of the human eye using magnetization transfer contrast enhancement, *Invest. Ophthalmol. Vis. Sci.* 41 (12) (2000) 3878–3881, Medline.
- [19] S.A. Strenk, J.L. Semmlow, L.M. Strenk, P. Munoz, J. Gronlund-Jacob, J.K. DeMarco, Age-related changes in human ciliary muscle and lens: a magnetic resonance imaging study, *Invest. Ophthalmol. Vis. Sci.* 40 (6) (1999) 1162–1169, Medline.
- [20] S. Krag, T.T. Andreassen, Mechanical properties of the human posterior lens capsule, *Invest. Ophthalmol. Vis. Sci.* 44 (2) (2003) 691–696, Medline.
- [21] S. Krag, T.T. Andreassen, Mechanical properties of the human lens capsule, *Prog. Retin. Eye Res.* 22 (6) (2003) 749–767, doi:10.1016/S1350-9462(03)00063-6.
- [22] M. Dubbelman, G.L. van der Heijde, H.A. Weeber, G.F. Vrensen, Changes in the internal structure of the human crystalline lens with age and accommodation, *Vis. Res.* 43 (22) (2003) 2363–2375, doi:10.1016/S0042-6989(03)00428-0.
- [23] M.V. Subbaram, J.C. Gump, M.A. Bullimore, R. Sooryakumar, The elasticity of the human lens, *Invest. Ophthalmol. Vis. Sci.* 43 (2002), E-Abstract 468, Abstract.
- [24] A.P. Beers, G. van der Heijde, Presbyopia and velocity of sound in the lens, *Optom. Vis. Sci.* 71 (4) (1994) 250–253, Medline.
- [25] F.A. Duck, Physical Properties of Tissue: A Comprehensive Reference Book, Academic Press, Harcourt Brace Jovanovich, Publishers, London, UK, 1990.
- [26] K.R. Heys, S.L. Cram, R.J. Truscott, Massive increase in the stiffness of the human lens nucleus with age: the basis for presbyopia? *Mol. Vis.* 10 (2004) 956–963, Medline.
- [27] A.S. Saada, Elasticity: Theory and Application, Pergamon Press Inc., Elmsford, NY, 1974.
- [28] D.P. Theret, M.J. Levesque, M. Sato, R.M. Nerem, L.T. Wheeler, The application of a homogeneous half-space model in the analysis of endothelial cell micropipette measurements, *J. Biomech. Eng.* 110 (3) (1998) 190–199, Medline.
- [29] R.F. Fisher, Elastic constants of the human lens capsule, *J. Physiol. (London)* 201 (1) (1969) 1–19, Medline.
- [30] G.W. van Alphen, W.P. Graebel, Elasticity of tissues involved in accommodation, *Vis. Res.* 31 (1991) 1417–1438, doi:10.1016/0042-6989(91)90061-9.
- [31] ABAQUS Version 6. 5, ABAQUS, Inc., Pawtucket, RI, 2005.
- [32] J.A. Tablbert, A.R. Parkinson, Development of an automatic, two-dimensional finite element mesh generator using quadrilateral elements and Bezier curve boundary definitions, *Int. J. Numer. Meth. Eng.* 29 (1990) 1551–1567.
- [33] T.D. Blacker, M.B. Stephenson, Paving: a new approach to automated quadrilateral mesh generation, *Int. J. Numer. Meth. Eng.* 32 (1991) 811–847, doi:10.1002/nme.1620320410.
- [34] C.K. Lee, S.H. Lo, A new scheme for the generation of a graded quadrilateral mesh, *Comput. Struct.* 52 (1994) 847–857, doi:10.1016/0045-7949(94)90070-1.
- [35] T.S. Lau, S.H. Lo, Generation of quadrilateral mesh over analytical curved surface, *Finite Elem. Anal. Des.* 27 (1997) 251–272, doi:10.1016/S0168-874X(97)00015-2.
- [36] Y.K. Lee, C.K. Lee, A new indirect anisotropic quadrilateral mesh generation scheme with enhanced local mesh smoothing procedures, *Int. J. Numer. Meth. Eng.* 58 (2003) 277–300, doi:10.1002/nme.771.
- [37] B.F. Belgacem, Y. Renard, L. Slimane, A mixed formulation for the Signirini problem in nearly incompressible elasticity, *Appl. Numer. Math.* 54 (2005) 1–22, doi:10.1016/j.apnum.2004.09.036.
- [38] C.E. Jones, D.A. Atchison, R. Meder, J.M. Pope, Refractive index distribution and optical properties of the isolated human lens measured using magnetic resonance imaging (MRI), *Vis. Res.* 45 (18) (2005) 2352–2366, doi:10.1016/j.visres.2005.03.008.

- [39] C.H. Chien, T. Huang, R.A. Schachar, Analysis of human crystalline lens accommodation, *J. Biomech.* 369 (4) (2006) 672–680, doi:10.1016/j.jbiomech.2005.01.017.
- [40] F.A. Bettelheim, M.J. Lizak, J.S. Zigler Jr., Synergetic response of aging normal human lens to pressure, *Invest. Ophthalmol. Vis. Sci.* 44 (1) (2003) 258–263, Medline.
- [41] R.A. Schachar, Letter to the editor: accommodation, presbyopia, and the lenticular synergetic response, *Curr. Eye Res.* 30 (11) (2005) 927, doi:10.1080/02713680500246965.
- [42] M.J. Hogan, J.A. Alvarado, J.E. Weddell, *Histology of the Human Eye*, W.B. Saunders Company, Philadelphia, PA, 1971.
- [43] J. Nordmann, G. Mack, G. Mack, Nucleus of the human lens: III. Its separation, its hardness, *Ophthalmic Res.* 6 (1974) 216–222.
- [44] J.M. Rakic, A. Galand, G.F. Vrensen, Separation of fibres from the capsule enhances mitotic activity of human lens epithelium, *Exp. Eye Res.* 64 (1) (1997) 67–72, doi:10.1006/exer.1996.0179.
- [45] I. Sakabe, T. Oshika, S.J. Lim, D.J. Apple, Anterior shift of zonular insertion onto the anterior surface of human crystalline lens with age, *Ophthalmology* 105 (2) (1998) 295–299, Medline.
- [46] R.F. Fisher, The force of contraction of the human ciliary muscle during accommodation, *J. Physiol. (London)* 270 (1) (1977) 51–74, Medline.
- [47] G.W. van Alphen, S.L. Robinette, F.J. Macri, Drug effects on ciliary muscle and choroid preparations in vitro, *Arch. Ophthalmol.* 68 (1962) 81–89, Medline.
- [48] H. von Helmholtz, *Über die akkommodation des auges*, *Arch. Ophthalmol.* 1 (1855) 1–74.
- [49] J.F. Koretz, C.A. Cook, P.L. Kaufman, Aging of the human lens: changes in lens shape upon accommodation and with accommodative loss, *J. Opt. Soc. Am. A Opt. Image Sci. Vis.* 19 (1) (2002) 144–151, Medline.
- [50] M. Dubbelman, G.L. Van der Heijde, H.A. Weeber, Change in shape of the aging human crystalline lens with accommodation, *Vis. Res.* 45 (1) (2005) 117–132, doi:10.1016/j.visres.2004.07.032.
- [51] T. Young, On the mechanism of the eye, *Philos. Trans. R. Soc. (London)* 92 (1801) 23–88.
- [52] M. Tscherning, *Physiological Optics*, 2nd ed., The Keyston, Philadelphia, PA, 1904.
- [53] E.F. Fincham, Mechanism of accommodation, *Br. J. Ophthalmol.* 8 (suppl) (1937) 2–80.
- [54] Y. Li, M.R. Chalta, D. Huang, Measurement of lens curvature change during accommodation with high-speed optical coherence tomography, *Invest. Ophthalmol. Vis. Sci.* 46 (2005), E-Abstract # 2554. Abstract.
- [55] D. Siedlecki, H. Kasprzak, B.K. Pierscionek, Schematic eye with a gradient-index lens and aspheric surfaces, *Opt. Lett.* 29 (11) (2004) 1197–1199, Medline.
- [56] R. Beauchamp, B. Mitchell, Ultrasound measures of vitreous chamber depth during ocular accommodation, *Am. J. Optom. Physiol. Opt.* 62 (8) (1985) 532–533.
- [57] W. Drexler, A. Baumgartner, O. Findl, C.K. Hitzenberger, A.F. Fercher, Biometric investigation of changes in the anterior eye segment during accommodation, *Vis. Res.* 37 (19) (1997) 2789–2800, doi:10.1016/j.jbiomech.2005.01.017.
- [58] L.A. Ostrin, A. Glasser, Comparisons between pharmacologically and Edinger–Westphal-stimulated accommodation in rhesus monkeys, *Invest. Ophthalmol. Vis. Sci.* 46 (2) (2005) 609–617, Medline.
- [59] A.E. Stadfeldt, Die veränderung der lines bei traction der zonula, *Klin. Monatsbl. Augenheilkd.* 34 (1896) 429–431.
- [60] B. Pierscionek, In vitro alteration of human lens curvatures by radial stretching, *Exp. Eye Res.* 57 (5) (1993) 629–635 [central steepening secondary to zonular traction is determined by calculating the radius of curvature at $x=0$ from the quadratic formulas given for the 27-year-old lens in Table 1]. doi:10.1006/exer.1993.1168.
- [61] R.A. Schachar, Qualitative effect of zonular tension on freshly extracted intact human crystalline lenses: implications for the mechanism of accommodation, *Invest. Ophthalmol. Vis. Sci.* 45 (8) (2004) 2691–2695, Medline.
- [62] J.C. He, S.A. Burns, S. Marcos, Monochromatic aberrations in the accommodated human eye, *Vis. Res.* 40 (1) (2000) 41–48.
- [63] S. Ninomiya, T. Fujikado, T. Kuroda, Y. Tano, T. Oshika, Y. Hirohara, T. Mihashi, Changes of ocular aberration with accommodation, *Am. J. Ophthalmol.* 134 (6) (2002) 924–926, doi:10.1016/S0002-9394(02)01703-8.
- [64] C.A. Hazel, M.J. Cox, N.C. Strang, Wavefront aberration and its relationship to the accommodative stimulus-response function in myopic subjects, *Optom. Vis. Sci.* 80 (2) (2003) 151–158, Medline.
- [65] R.A. Schachar, Cause and treatment of presbyopia with a method for increasing the amplitude of accommodation, *Ann. Ophthalmol.* 24 (12) (1992) 445–449, 452 (Medline).
- [66] R.A. Schachar, T. Huang, X. Huang, Mathematic proof of Schachar's hypothesis of accommodation, *Ann. Ophthalmol.* 25 (1) (1993) 5–9, Medline.
- [67] R.A. Schachar, Is Helmholtz's theory of accommodation correct? *Ann. Ophthalmol.* 31 (1999) 10–17, <http://www.2ras.com/15.pdf>.
- [68] J.L. Demer, R. Kono, W. Wright, Magnetic resonance imaging of human extraocular muscles in convergence, *J. Neurophysiol.* 89 (4) (2003) 2072–2085, Medline.
- [69] R.A. Schachar, T.D. Black, R.L. Kash, D.P. Cudmore, D.J. Schanzlin, The mechanism of accommodation and presbyopia in the primate, *Ann. Ophthalmol.* 27 (1995) 58–67, <http://www.2ras.com/8.pdf>.
- [70] R.A. Schachar, F. Kamangar, Computer image analysis of ultrasound biomicroscopy of primate accommodation, *Eye* 20 (2006) 226–233, doi:10.1038/sj.eye.6701838.
- [71] R.A. Schachar, C. Tello, D.P. Cudmore, J.M. Liebmman, T.D. Black, R. Ritch, In vivo increase of the human lens equatorial diameter during accommodation, *Am. J. Physiol. Regul. Integr. Comp. Physiol.* 271 (3 Pt 2) (1996) R670–R676, Medline.
- [72] R.S. Wilson, Does the lens diameter increase or decrease during accommodation? Human accommodation studies: a new technique using infrared retro-illumination video photography and pixel unit measurement, *Trans. Am. Ophthalmol. Soc.* 95 (1997) 261–270, Medline.
- [73] A. Glasser, P.L. Kaufman, The mechanism of accommodation in primates, *Ophthalmology* 106 (5) (1999) 863–872, Medline.
- [74] G. Baikoff, E. Lutun, J. Wei, C. Ferraz, Anterior chamber optical coherence tomography study of human natural accommodation in a 19-year-old albino, *J. Cataract Refract. Surg.* 30 (3) (2004) 696–701, Medline.
- [75] A. Glasser, M. Wendt, L. Ostrin, Accommodative changes in lens diameter in rhesus monkeys, *Invest. Ophthalmol. Vis. Sci.* 47 (1) (2006) 278–286, Medline.
- [76] N.S. Levy, Comparing MRIs with movement artifact, eLetter, *Invest. Ophthalmol. Vis. Sci.*, 2000, <http://www.iovs.org/cgi/eletters/40/6/1162>.
- [77] N.S. Levy, The mechanism of accommodation in primates, letter to the editor, *Ophthalmology* 107 (4) (2000) 625–626, Medline.
- [78] R.A. Schachar, References are required for measurement of OCT images, letter to the editor, *J. Cataract Refract. Surg.* 31 (2) (2005) 257–258.
- [79] R.A. Schachar, F. Kamangar, Proper controls are required for accommodative experiments. 2006, <http://www.iovs.org/cgi/eletters/47/1/278-314>.
- [80] R.A. Schachar, F. Kamangar, Addition controls required for assessing in vivo accommodation, eLetter, *Invest.*

- Ophthalmol. Vis. Sci., 2006, published online, <http://www.iovs.org/cgi/eletters/47/3/1076>.
- [81] R.H. Marmer, Movement of the lens during accommodation, eLetter, Invest. Ophthalmol. Vis. Sci., 2006, published online, <http://www.iovs.org/cgi/eletters/47/1/278-310>.
- [82] R.H. Marmer, Upward lens movement not explained by eye movement, eLetter, Invest. Ophthalmol. Vis. Sci. (2006), in press.
- [83] N.S. Levy, Alternative interpretation of the age-related decrease in circumlental space, eLetter, Invest. Ophthalmol. Vis. Sci., 2006, published online, <http://www.iovs.org/cgi/eletters/47/3/1087>.
- [84] N. Brown, The shape of the lens equator, Exp. Eye Res. 19 (6) (1974) 571–576, 10.1016/0014-4835(74)90094-3.
- [85] M.W. Neider, K. Crawford, P.L. Kaufman, L.Z. Bitto, In vivo videography of the rhesus monkey accommodative apparatus. Age-related loss of ciliary muscle response to central stimulation, Arch. Ophthalmol. 108 (1) (1990) 69–74, Medline.
- [86] K. Ludwig, E. Wegscheider, J.P. Hoops, A. Kampik, In vivo imaging of the human zonular apparatus with high-resolution ultrasound biomicroscopy, Graefes Arch. Clin. Exp. Ophthalmol. 237 (5) (1999) 361–371, 10.1007/s004170050245.
- [87] J.M. Vanderploeg, Near visual acuity measurements of space shuttle crewmembers, Aviat. Space Environ. Med. 57 (1985) 492.
- [88] R.A. Schachar, D.P. Cudmore, The effect of gravity on the amplitude of accommodation, Ann. Ophthalmol. 26 (3) (1994) 65–70, Medline.
- [89] A. Sokolowska, F. Thorn, Accommodation induced changes in crystalline lens position, Invest. Ophthalmol. Vis. Sci. 44 (2003), E-Abstract # 4072. Abstract.
- [90] R.A. Schachar, A.J. Bax, Mechanism of human accommodation as analyzed by nonlinear finite element analysis, Comp. Ther. 27 (2) (2001) 122–132, Medline.
- [91] W.V. Shung, An analysis of a crystalline lens subjected to equatorial periodic pulls, Ph.D. dissertation, University of Texas at Arlington, Arlington, TX, 2002.
- [92] P.N. Farnsworth, P. Burke, Three-dimensional architecture of the suspensory apparatus of the lens of the Rhesus monkey, Exp. Eye Res. 25 (6) (1977) 563–576, Medline.
- [93] B.W. Streeten, in: F.A. Jakobiec (Ed.), Zonular Apparatus, Ocular Anatomy Embryology and Teratology, Harper and Row, Philadelphia, PA, 1982, pp. 331–353.
- [94] H.J. Burd, G.S. Wilde, S.J. Judge, Can reliable values of Young's modulus be deduced from Fisher's (1971) spinning lens measurements? Vis. Res. 46 (8–9) (2006) 1346–1360, doi:10.1016/j.visres.2005.07.012.
- [95] C. Kelman, in: N. Jaffe (Ed.), Phacoemulsification, Cataract Surgery and its Complications, 2nd ed., C.V. Mosby Company, St. Louis, MO, 1976.
- [96] J.L. Alio, P. Schimchak, H.P. Negri, R. Montes-Mico, Crystalline lens optical dysfunction through aging, Ophthalmology 112 (11) (2005) 2022–2029, doi:10.1016/j.ophtha.2005.04.034.
- [97] H.A. Weeber, G. Eckert, F. Soergel, C.H. Meyer, W. Pechhold, R.G. van der Heijde, Dynamic mechanical properties of human lenses, Exp. Eye Res. 80 (3) (2005) 425–434, doi:10.1016/j.exer.2004.10.010.
- [98] R.A. Schachar, Comment on "Dynamic mechanical properties of human lenses," By H.A. Weeber et al. [Experimental Eye Research. 2005;80(3):425–434], Exp. Eye Res 81 (2) (2005) 236, doi:10.1016/j.exer.2005.03.016.
- [99] G. Heron, W.N. Charman, C. Schor, Dynamics of the accommodation response to abrupt changes in target vergence as a function of age, Vis. Res. 41 (4) (2001) 507–519, Medline.
- [100] G. Heron, W.N. Charman, C.M. Schor, Age changes in the interactions between the accommodation and vergence systems, Optom. Vis. Sci. 78 (10) (2001) 754–762, Medline.
- [101] J.A. Mordi, K.J. Ciuffreda, Dynamic aspects of accommodation: age and presbyopia, Vis. Res. 44 (6) (2004) 591–601, Medline.
- [102] R.A. Schachar, Age related changes in accommodative dynamics in humans. Letter to the Editor. Vis. Res. (2006), in press, doi:10.1016/j.visres.2006.03.025.
- [103] H.R. Saber, T.J. Butler, D.G. Cottrell, Resistance of the human posterior lens capsule and zonules to disruption, J. Cataract Refract. Surg. 24 (4) (1998) 536–542, Medline.
- [104] J.F. Koretz, C.A. Cook, P.L. Kaufman, Aging of the human lens: changes in lens shape at zero-diopter accommodation, J. Opt. Soc. Am. A Opt. Image Sci. Vis. 18 (2) (2001) 265–272, Medline.
- [105] R.A. Schachar, Growth patterns of fresh human crystalline lenses measured by in vitro photographic biometry, J. Anat. 206 (6) (2005) 575–580, Medline.
- [106] K.J. Al-Ghoul, R.K. Nordgren, A.J. Kuszak, C.D. Freel, M.J. Costello, J.R. Kuszak, Structural evidence of human nuclear fiber compaction as a function of ageing and cataractogenesis, Exp. Eye Res. 72 (3) (2001) 199–214, Medline.
- [107] T. Fujikado, T. Kuroda, S. Ninomiya, N. Maeda, Y. Tano, T. Oshika, Y. Hirohara, T. Mihashi, Age-related changes in ocular and corneal aberrations, Am. J. Ophthalmol. 138 (1) (2004) 143–146, Medline.
- [108] P. Artal, E. Berrio, A. Guirao, P. Piers, Contribution of the cornea and internal surfaces to the change of ocular aberrations with age, J. Opt. Soc. Am. A Opt. Image Sci. Vis. 19 (1) (2002) 137–143, Medline.